ACS chemical biology

Articles

pubs.acs.org/acschemicalbiology

Structure, Dynamics, and Activity of Xylanase Solvated in Binary Mixtures of Ionic Liquid and Water

Vance W. Jaeger and Jim Pfaendtner*

Department of Chemical Engineering, University of Washington, Seattle, Washington 98195, United States

Supporting Information

ABSTRACT: We have discovered that a family 11 xylanase from *Trichoderma longibrachiatum* maintains significant activity in low concentrations of the ionic liquids (IL) 1-ethyl-3-methyl-imidazolium acetate ([EMIM][OAc]) or 1-ethyl-3-methyl-imidazolium ethyl sulfate ([EMIM][$EtSO_4$]) in water. In order to understand the mechanisms by which the ionic liquids affect the activity of xylanase, we conducted molecular dynamics simulations of the enzyme in various concentrations of the cosolvent. The simulations show that higher concentrations of ionic liquid correlate with less deviation from the starting crystallographic structure. Dynamic motion of the protein is severely dampened by even the lowest tested concentrations of ionic liquid as measured by root-mean-square fluctuation. Principal component analysis shows that the characteristics of the main modes of enzyme motion are greatly affected by the choice of solvent. Cations become kinetically trapped in the binding pocket, allowing them to act as a competitive inhibitor to the natural substrate. Dynamic light scattering and kinetic studies evaluated the stability of the enzyme in the new solvents. These studies indicate that likely factors in the loss of enzyme activity for this xylanase are the dampening of dynamic motion and kinetic trapping of cations in the binding pocket as opposed to the denaturing of the protein.

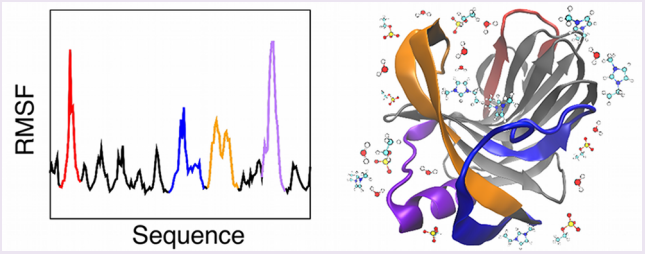

Hemicellulose, a major component of biomass, can be hydrolyzed into monosaccharides for fermentation or catalytic upgrading. Xylan, a common hemicellulose, is typically hydrolyzed into constituent xylose subunits by one of two methods that decompose the crucial β-1,4-glycosidic bond either by high temperature acid-catalyzed decomposition[1] or by enzymatic decomposition using a β-1,4-xylanase. The latter requires more costly enzymes but uses less energy and produces less caustic waste.

In both approaches the use of ionic liquids for pretreatment of cellulosic feedstock, which includes hemicelluloses and lignins, has been thoroughly explored. Ionic liquids are organic salts with melting points below 100 °C. They can solvate the complex mixtures of cellulose, hemicellulose, and lignin contained in the biomass of interest.[2,3] By solvating biomass using ionic liquids, more area is exposed for attack by the enzyme, and the reaction proceeds much more quickly.[4] However, a key challenge remains in that the IL and expanded biomass are typically separated prior to enzymatic processing to break down the polysaccharide.

Certain biomass-degrading enzymes have been shown to remain active in binary mixtures of water and organic solvents,[5] while some other classes of enzymes have displayed unique characteristics in pure organic solvents.[6] Hyperthermophilic cellulases, for example, have been found to maintain complete activity in levels of up to 20% (v/v) ionic liquid in water.[7] This is counterintuitive, since one might expect a charged solvent of high ionic strength to disrupt the hydrogen bonding patterns of a well-formed enzyme and lead to loss of activity by loss of higher order structure. Moreover, a more viscous medium might be expected to reduce product yield, but this is not always true.[8] Still, the aqueous-IL solvated enzyme performs relatively well even during experiments on the time scale of hours. Other proteins have been shown to maintain higher order structuring in concentrations of ionic liquid in the range of 20−25% (v/v) ionic liquid in water,[9,10] indicating they have not denatured. Molecular simulation of the solvated enzyme can provide molecular-scale details complementary to modern experimental techniques and indicate the properties of the enzyme and solvent that lead to activity loss. The tools of molecular simulation have been used to study interactions of ILs and cellulose[11−13] but have seen limited application to IL/enzyme interactions.[14]

Molecular simulation could be used to provide new insight and complement experiments with atomic-scale understanding of the enzyme/solvent interactions. Mechanistically, explanations for the IL-induced reduction in apparent reaction rates include solvent/substrate effects, competitive inhibition, enzyme solvation, and disruption of enzyme structure. All of these could contribute to changes in the dynamic motions of the enzyme, interfere with the active site, or affect conformational changes related to the enzymatic mechanism. Evidence suggests that some dynamic motions are related to ligand

Received: December 11, 2012
Accepted: March 21, 2013
Published: March 21, 2013

   dx.doi.org/10.1021/cb3006837 | ACS Chem. Biol. 2013, 8, 1179−1186

binding, catalytic activity, and thus apparent reaction rates in general.[15,16] However, this is a vigorous topic of discussion in the literature, and the role of dynamics in enzyme activity continues to be debated.[17] Herein we refer to dynamic motions as those studied on time scales of 50−500 ns using molecular simulations. For biomolecules of the size studied in this work this time scale is not sufficient to probe large-scale structural change, in essence limiting discussion to local conformational changes.

Family 11 glycoside hydrolases (GH11), such as the one we have tested, have been extensively studied both experimentally and computationally in water. Therefore there exists a wealth of quantitative and qualitative data for comparison to new studies in ionic liquids. Previous work has revealed connections between the structure of the protein and its enzymatic activity. The shape of the enzyme (Figure 1) is analogous to a left hand

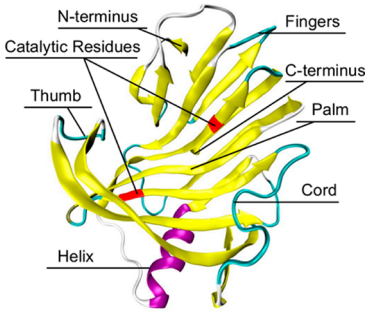

Figure 1. Family 11 xylanase from *Trichoderma longibrachiatum*. Colored according to secondary structure. Catalytic residues are in red.

with the characteristics of a thumb, fingers, palm, cord, and a single α-helical region. The thumb has been shown to have a profound effect on the binding and cleaving of the substrate.[18,19] The fingers constitute the bulk of the binding pocket. The palm is the location of the catalytic glutamate and glutamic acid.[20] The cord regulates the entrance of substrate into the binding pocket, and stabilizing mutations of the α helix have been shown to increase the thermal stability of the enzyme.[21] Additionally, one study compared several similar xylanases to the specific one studied herein to find the properties that indicate higher thermophilicity.[22] Other computational studies have shown that even at short time scales molecular dynamics (MD) simulations perform well in predicting the relative thermal stability of family 11 xylanases.[23]

To address our significant gap in understanding of the mechanisms by which ILs change the activity of glycoside hydrolases, we have undertaken an extensive computational study. Our representative GH11 enzyme, xylanase II from *Trichoderma longibrachiatum*, was studied by systematically changing the IL type, the concentration of the IL−water solution, and the temperature of our simulations. Approximately 4.6 μs of atomic resolution MD simulation was performed at temperatures ranging from 310 to 363 K. We complement the simulations with experimental findings that demonstrate partial retention of activity and retention of structure in multiple IL−water solutions.

RESULTS AND DISCUSSION

Determining Xylanase Activity in IL. The enzyme maintained significant activity in both [EMIM][$EtSO_4$] and [EMIM][OAc] (Figure 2). Incubation in low concentrations of

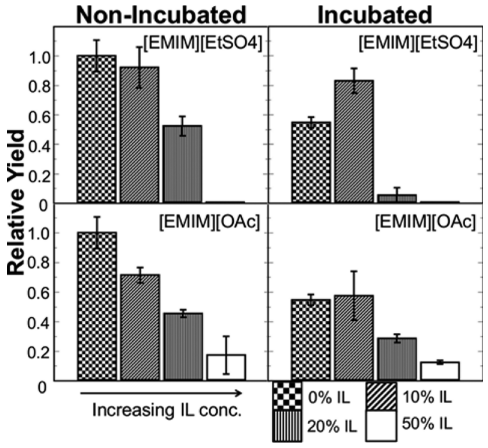

Figure 2. Experimental yield of xylose. Xylanase in systems containing ionic liquid with and without substrate-free incubation. Relative yield measured versus a baseline of the non-incubated water system. Error bars are the standard deviation of six measurements (three independent samples measured in duplicate).

ionic liquid does not adversely affect the yield when compared to the loss in yield for the analogous aqueous system. In fact, for the lowest tested concentration of IL, the [EMIM][$EtSO_4$] incubated system yields more xylose as product than the water incubated system. The relationship between product yield and IL concentration is not simply linear. Additionally, we observed increased turbidity over the timespan of the experiment for some IL-containing systems, which could be caused by the aggregation of the enzyme. This hypothesis is tested by DLS in the following section.

Effect of IL on Xylanase Structure. An analysis of the root-mean-square deviation (RMSD) of the Cα atoms indicates that the systems with higher concentrations of ionic liquid generally maintain closer agreement to the experimentally determined crystal structure of the enzyme over the time scale studied (Figure 3A,B). Kinetic trapping has been a problem reported by other researchers simulating enzymes in IL on the time scale of up to 20 ns.[14] Yet these trends hold over the full range of variables tested and over replicate simulations. Loops in particular begin to transition between similar but different folded states. Even at elevated temperatures of up to 363 K, highly ionic systems show few signs of denaturing or disruption of higher order structuring. Two of the most interesting features in the simulations occur at elevated temperatures. First, as the temperature increases for the aqueous system, the fluctuations near the helix (Thr152 to Gln162) increase in magnitude. This behavior may explain the loss of activity at high temperatures for similar GH11 proteins and the increased stability afforded by stabilizing mutations in the helix as shown by Turunen and co-workers,[35] who added a disulfide bridge near the N-terminus of the helix by mutating Ser110 and Asn154 to cysteine. Second, in the highest temperature system, 20 wt % [EMIM][$EtSO_4$], the fluctuations around the thumb (Gln121 to Thr133) become very large compared to the rest of the system and compared to its counterpart in 20 wt % [EMIM][OAc]. In addition, the distance between the fingers and the thumb increases. This behavior may indicate an approaching limit of stability for the system and predict a severe loss in enzyme activity near this concentration.

Several simulations were extended to 500 ns of simulation time in order to obtain more sampling of conformational

dx.doi.org/10.1021/cb3006837 | *ACS Chem. Biol.* 2013, 8, 1179−1186

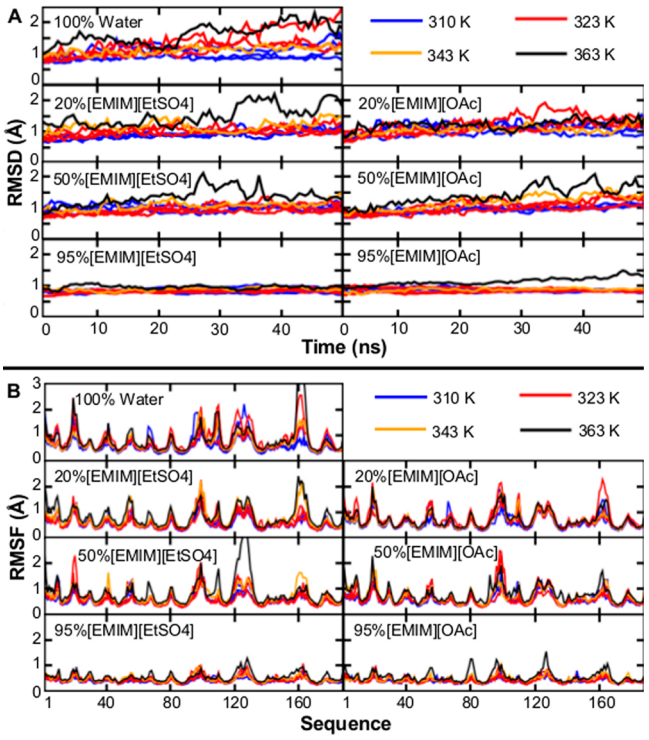

Figure 3. Root mean square deviation (RMSD) (A) and fluctuation (RMSF) (B) of xylanase alpha carbons across a range of cosolvent concentrations and temperatures. Triplicate simulations at 310 and 323 K are shown.

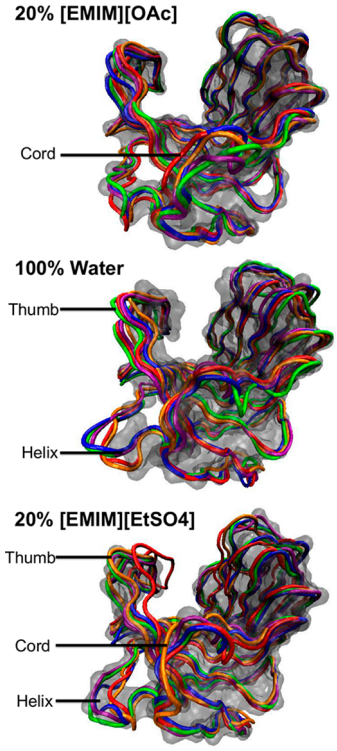

Figure 4. Snapshots of the molecular dynamics trajectories (310 K). Areas of interest are indicated. Gray cloud (minimized structure). Red (100 ns). Orange (200 ns). Green (300 ns). Blue (400 ns). Violet (500 ns).

changes in the enzyme (Supplementary Table 2). The results from 50 ns are similar at a time scale 10 times longer. The enzyme remained stable in IL, as measured by RMSD, which never exceeded 2 Å on a Bezier smoothed plot (Supplementary Figure 2). On this time scale, systems of 20 wt % IL and the water system show similar displacement from the crystallographic structure. Figure 4 contains snapshots of the systems at 100 ns intervals and highlights the features of each system that deviate the most from the experimentally determined structure. The cord was the most active of the main features. This was likely due to its interactions with the cation. Moreover, in water at the elevated temperature of 363 K, the enzyme did not have an RMSD greater than 3 Å. The residues following the N-terminus of the helix showed particularly high thermal activity compared with the rest of the protein. More specific differences between these systems are discussed in the following sections.

In addition to studying the atomic-scale details of GH11 at the submicrosecond time scale, we probed the solvent-induced features using light scattering, which can be used to roughly estimate changes in the size of the enzyme and its aggregates. Use of more direct measurements of the protein structure (e.g., circular dichroism) in ILs is confounded by the absorbance spectrum of the ions.[36] We employed DLS to gain semi-quantitative insights into whether the enzyme is undergoing aggregation or large-scale denaturation in ionic solvents. Other scattering techniques, such as SAXS and SANS, have shown that other proteins maintain much of their secondary and tertiary structure in ionic liquid concentrations of up to 20% (v/v).[37] The measurement of particle size with this approach is very sensitive to the parameters of refractive index and viscosity of the solvent. We interpolated these data from previously reported values across both temperature and composition and therefore use the DLS results primarily to gain mostly qualitative insights.

The enzyme's hydrodynamic radius was measured before and after incubation across the range of concentrations studied by simulation and in 8 M urea (Table 1). We interpreted the data to determine the presence or absence of proteins near their aqueous hydrodynamic radius (of about 2 nm) and the presence of much larger aggregates. Additionally, the samples were inspected for turbidity that would also indicate large aggregates. DLS indicates that the buffered aqueous system maintains most of its protein near its native state even after incubation, and no turbidity is apparent in either the DLS or the kinetic studies. At the same time, incubation of the enzyme led to a more than 40% drop in the yield of product for the kinetic studies (cf., Figure 2). Two possibilities to explain the seemingly apparent contradiction are that either (a) the structural changes leading to loss in activity are too small to be detected by DLS or (b) the native protonation state of the lyophilized enzyme used in the kinetic studies was changed from a more optimal state to a less optimal state after incubation. In the first case, a more sensitive scattering method could be used. In the second case, we observe that 10 wt % [EMIM][$EtSO_4$] affords some protection from this loss in activity even though its pH of 8.1 is farther from the optimum of about 5.5 suggested by the manufacturer. The presence of small amounts of sulfuric acid, hydrogen sulfide, and ethanol, which are the products of the slow degradation of [$EtSO_4$] in water,[38,39] could lead to a more primed state for the protonated catalytic residue.

Interestingly, DLS indicates that there is a critical range of concentrations of IL where aggregation occurs. Using [EMIM]-[$EtSO_4$] as an example, at a concentration of 10 wt %,

dx.doi.org/10.1021/cb3006837 | ACS Chem. Biol. 2013, 8, 1179–1186

Table 1. Dynamic Light Scattering Analysis of Xylanase[a]

	no incubation			48 h incubation		
	R_h (nm)	width (nm)	turbid ?	R_h (nm)	width (nm)	turbid ?
100% water	1.91	0.70	no	1.72	0.59	no
10% [EMIM][OAC]	1.75	0.58	no	1.44	0.32	no
10% [EMIM][$EtSO_4$]	1.61	0.36	no	1.60	0.43	no
20% [EMIM][OAC]	1.93	0.53	no	1.65	0.30	no
20% [EMIM][$EtSO_4$]	1.64	0.51	no	33.59	6.64	yes
50% [EMIM][OAC]	56.63	18.48	yes	51.68	12.89	yes
50% [EMIM][$EtSO_4$]	26.43	7.58	yes			yes
95% [EMIM][OAC]	1.10	0.20	no	3.65	0.59	no
95% [EMIM][$EtSO_4$]	2.11	1.33	no	1.76	0.47	no
8 M urea	2.11	0.46	no	3.36	0.74	no

[a]Enzyme solvated in various wt % concentrations of two ionic liquids, water, and urea. Hydrodynamic radius (R_h) and peak width are taken from an average of measured peaks below 250 nm.

aggregation is not detected by DLS or by turbidity either before or after incubation. Conversely, at 20 wt % aggregation is not detected immediately. At 50 wt %, aggregation is very rapid, and the aggregates or the incubated sample are large enough to be completely filtered, yielding no measurement of protein in the sample. We were unable to determine whether these aggregates were multimers of natively folded enzyme or if they are constituted of unfolded enzyme. At the highest tested concentration of 95 wt % IL, the enzyme displays a normal hydrodynamic radius and no aggregation is detected by DLS or by turbidity. The formation of large protein aggregates is not generally accessible with atomistic MD simulations due to scale limitations in both size and time, but insights into the propensity for aggregation can be gained through the investigation of solvent−protein interactions displayed in the simulation.

In the simulations we observed unique interactions between the anion and the positively charged surface residues of the enzyme. Specifically, lysine and arginine tend to attract the negatively charged oxygen atoms of acetate and ethyl sulfate. White and co-workers have suggested that charged surface residues, specifically lysine and glutamic acid, help deter nonspecific interactions including aggregation.[40] Therefore, interruption of the environment around these charged residues may lead to higher levels of aggregation, as in the case of [EMIM][$EtSO_4$] but not in the case of [EMIM][OAc]. The average number of anion-oxygen atoms within 4 Å of lysine, arginine, or histidine was tracked over the length of the 500 ns simulations for 20 wt % solutions of both [EMIM][OAc] and [EMIM][$EtSO_4$]. For acetate, 15 ± 5 oxygen atoms occupied the space, while for ethyl sulfate, 27 ± 7 occupied the space. High concentrations of these anions around the positively charged residues may also facilitate the salt bridging of separate proteins and encourage aggregation. On the other hand, the simulations do not indicate an affinity of the cations for the negatively charged residues, which we expect is caused by much greater charge delocalization on the cation compared to the anions.

Changes in Structure and Dynamics. In order to quantify the magnitude of deviation from the average position for specific sites along the backbone of the enzyme, the root-mean-square fluctuation (RMSF) of the C_α atoms in the enzyme was computed. First, the RMSF was calculated over an equilibrated sample of each trajectory in order to identify regions of interest. We observed that the regions of highest fluctuation for the enzyme in water match the features of the enzyme that have been previously identified as important to enzymatic activity. The main features of the enzyme's Cα RMSF (Figure 3C,D) are centered about the following residues: the thumb, Arg128; the α helix, Asn157; the fingers His22, Ser42, Gly70, and Ser181; the cord, Pro98. The palm constitutes most of the remainder of the structure. Four of the five main features (the thumb, the α helix, the fingers, and the cord) show the highest levels of fluctuation in 100% water. These regions have specifically been implicated in the proper binding of the substrate and the release of the product.[41−43] A larger dynamic range of these features may help the protein move the substrate to its proper binding site and eject the product from the binding pocket. The fifth region is the palm, which is the active site of GH11 xylanase. Since biocatalytic activity requires careful arrangement of the catalytic side chains, large-scale fluctuations within this region could conceivably affect reaction rates.

In addition to the average fluctuations in an equilibrated portion of each simulation, we used the simulations that were extended to 500 ns to study how the fluctuations changed over time. The RMSF was measured around the arithmetic average structure over 1-ns windows (Supplementary Figure 3). In the aqueous systems, the temporal RMSF plots show activity in the region between the thumb and the cord that is notably less pronounced in the two ionic systems. As detailed below, we observed that some simulations with IL show the presence of a cation trapped near the chord. This might disrupt the natural motion of the chord region observed in aqueous simulations. The same windowed RMSF analysis was performed for the entire set of data, including the 50-ns runs. Even at the highest tested temperatures of 363 K, the ionic systems do not display the same characteristic fluctuations as the aqueous system. At this temperature, the aqueous protein fluctuates with a greater magnitude, and the ionic systems are still much more rigid.

Multiple researchers have implicated the dynamic motions of enzymes as being a key to their activity.[44] By moving in a semicoordinated fashion and specifying the distribution of states that the side chains occupy, the enzyme can (a) efficiently bind substrate, (b) direct it toward the catalytic site, (c) possibly aid in the chemical reaction by inducing new geometries or electronic structures that stabilize transition states, and (d) release the product. The introduction of a new solvent, when it does not denature the protein or cause kinetic trapping, can interrupt this order and disrupt any of the steps along this process, thereby leading to changes in activity and yield of product. In the following section, solvent-induced

dx.doi.org/10.1021/cb3006837 | ACS Chem. Biol. 2013, 8, 1179−1186

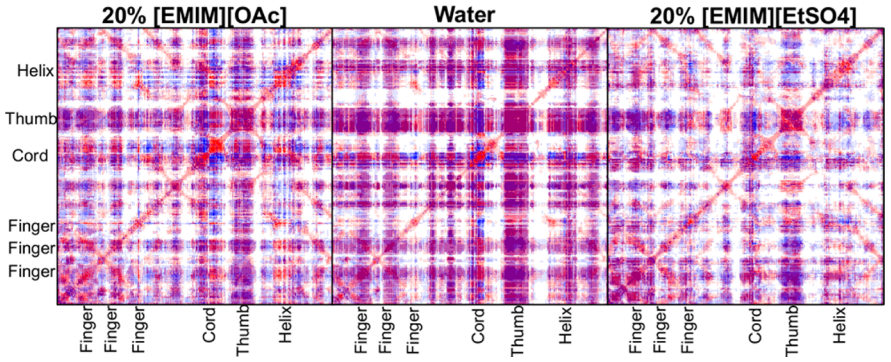

Figure 5. Covariance matrices of xylanase. Backbone motion in ionic liquids in xyz resolution. Red pixels are correlated, and blue are anti-correlated.

changes in the dynamics of the enzyme and in the coordination of its residues' motions will be discussed. This assumes that the system is at a new equilibrium state in the IL systems and that it is not kinetically trapped.

Principal Component Analysis. Using principal component analysis (PCA), the MD trajectories at 310 K were projected onto representative sets of eigenvectors in order to gain insight into the slow modes of motion. We used PCA study effect of solvents on correlated and anti-correlated motions in the enzyme. The covariance matrices were calculated for systems containing the lowest simulated concentrations of ionic liquid versus one of a purely aqueous system (Figure 5). As can be seen in the ionic systems, correlated motions are not completely preserved. Differences can be seen in the location of the regions of correlation as well as the size of the spans containing correlated motions. We would not expect the modes to completely disappear as the enzyme does retain activity in the IL solvent. Moreover, regions displaying little correlation in the aqueous system, such as region spanning the thumb and the helix, show more pronounced correlation and anti-correlation in the ionic systems. This potentially affects the ability of the enzyme to carry out its function as discussed above.

Next the PCA modes were visually represented via porcupine plots by projecting the first and second eigenvectors onto the alpha carbons of the protein backbone (Figure 6). In order to confirm that these modes are significant, the contribution of each mode was plotted (Supplementary Figure 4). For each of the samples taken in equilibrated regions of the trajectory, as determined by inspection of RMSD, systems with higher concentrations of ionic liquid display disrupted motion. The vectors are different in orientation, and the ordering of primary, secondary, and higher modes of motion from the aqueous systems is not maintained. Inspection of the trajectory of the aqueous systems reveals a shuffling motion of the hand-like enzyme as the thumb and fingers move in concert, as depicted by the dominant PCA mode in Figure 6. Conversely, the addition of IL changes this, and a new dominant mode takes over. The dominant motion is a slow opening and closing of the hand-like structure, which accounts for a large portion of the displacement from the crystal structure. The dominant mode in the aqueous system is preserved in the IL but is consistently present with a noticeably higher eigenvalue in the aqueous system. This is consistent with our expectations, as any motions related to enzymatic function would need to be preserved in the IL since it shows activity experimentally. We observed these effects over all 100-ns windows of analysis we investigated from the long 500-ns trajectories.

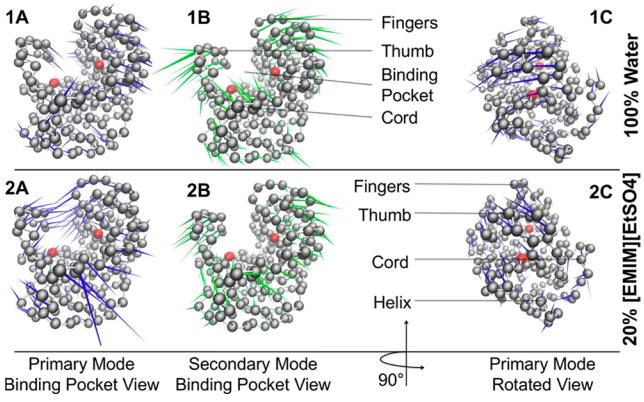

Figure 6. Principle components of xylanase motion. The aqueous enzyme (1A, 1B, 1C) is compared to its counterpart in 20 wt % [EMIM][$EtSO_4$] (2A, 2B, 2C). Columns A and B displays a view through the binding pocket, and column C displays a rotated view. Primary modes are blue, and secondary are green. Catalytic residues are red.

Competitive Inhibition from Cations. Since the active site is charged, we next investigated whether the strong interactions between solvent and catalytic residue could disrupt the catalytic cycle. The large number of possible instigators for the loss of enzymatic activity in these systems makes the task of experimentally verifying and measuring inhibition difficult by conventional means such as double reciprocal plots. The simulation trajectories were analyzed for the presence of organic ions in the binding pocket. For simulations containing either of the ILs, two or three cations preferentially occupy space very near the binding pocket (Figure 7). We observed

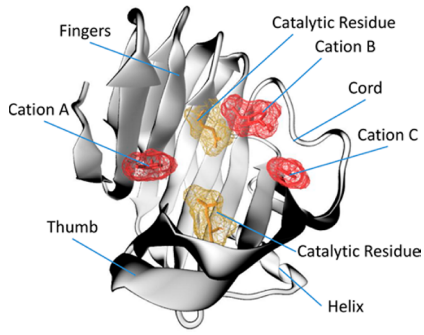

Figure 7. Kinetically trapped cations in the xylanase binding pocket. Catalytic residues are yellow. Cations are red.

dx.doi.org/10.1021/cb3006837 | *ACS Chem. Biol.* 2013, 8, 1179–1186

this for all concentrations and temperature ranges investigated in this study. The cation is roughly similar in shape and size to the enzyme's natural product of xylose, but the composition of the imidazolium ring differs very much from that of the xylose ring. It is therefore interesting to note that, during the inspection of the trajectories, it was incredibly rare for either of the first two cations to exit the binding region once they have become bound; they become kinetically trapped, at least on the 50−500 ns time scale. On the rare occasion that a cation leaves the binding pocket, it is quickly replaced by another cation. Because of how quickly the pocket became inhabited with cations at the beginning of the simulation, and because of the observed low likelihood of cations leaving the pocket over the time scales studied, competitive inhibition could play a role in the loss of activity.

No kinetically trapped anions were observed. As for the crystallographic waters, they leave the surface quickly. Yet, if the number of water molecules near the surface is tracked as a function of time, most IL-containing simulations converge to a similar number of molecules and then slightly fluctuate from there (Supplementary Figure 5). Exclusion of water from the catalytic site is also not observed.

Conclusion. The activity, stability, and dynamics of a family 11 glycoside hydrolase solvated in mixtures of ionic liquid and water were characterized by molecular simulation and experiment. Several hypotheses for the partial deactivation the enzyme were tested. Analysis of simulations and experimental data lead to several observations about the interactions of IL with this enzyme.

1. GH11 from *T. longibrachiatum* solvated in higher concentrations of ILs generally remains more stable with respect to its crystal structure than when solvated in water on the time scales studied.

2. The solvent environment of IL-containing systems causes fluctuations of the enzyme to be muted when compared to a purely aqueous system.

3. Natural correlated motions of the enzyme are not preserved as concentration of IL is increased.

4. [EMIM] binds strongly in the binding pocket, potentially reducing activity by inhibition.

5. Aggregation must be considered when mixing enzymes and ILs.

Future work in this area should decouple the role of the ionic strength and viscosity of the solutions; both simulation and experiment offer possible routes to do so. Our work also suggests that more insights are needed into the role of cations in the substrate binding pocket.

METHODS

Enzyme Simulations. All simulations were performed using widely accepted techniques with AMBER-compatible force fields implemented in NAMD2.7b3[24] with TIP3P[25] water. Protein forces were calculated using AMBER99sb,[26] and ionic liquid force fields were developed with the generalized amber force field (GAFF)[27] using point charges calculated by RESP[28] (Supplementary Figure 1, Supplementary Table 1). The van der Waals cutoff was set to 12 Å with a switching function implemented at 10 Å. Electrostatic interactions were treated with particle mesh Ewald summation using a mesh size of 1 Å. Constraining intramolecular hydrogen bond lengths with the SHAKE algorithm[29] permitted a time step of 2 fs. Temperature and pressure were regulated with a Langevin thermostat and a Nosé-Hoover Langevin piston barostat with a dampening coefficient of 0.5 ps^{-1} and a piston decay period of 2 ps. Replicate simulations were performed by reinitializing velocities from minimized structures. More details about the simulations and verification of the force field are included in the Supporting Information.

We selected xylanase from *Trichoderma longibrachiatum* (PDB ID: 3AKP)[30,31] as the model system. The first of the two chain sequences provided in the PDB file was used for all simulations. Crystallographic waters were maintained. We selected the ionic liquids (a) because of the ability of established force fields to reproduce experimental data for similar structures, (b) so that we could compare the results to other experimental studies of glycoside hydrolases in IL,[5,7] and (c) because of the promising abilities of [EMIM][OAc] as a solvent for cellulosic biomass.[32]

Xylose Yield. Xylanase from *Trichoderma longibrachiatum*, xylan from birchwood, 1-ethyl-3-methylimidazolium acetate [EMIM][OAc] (90% purity), and 1-ethyl-3-methylimidazolium ethyl sulfate [EMIM]-[$EtSO_4$] (95% purity) were purchased from Sigma Aldrich. Premixed concentrated PBS buffer was obtained from Calbiochem and diluted to a concentration 150 mM. Enzymatic hydrolysis of xylan was carried out in 5 g of solution with varying concentrations of ionic liquid in buffer. For all experiments, 1 mg of enzyme was rehydrated in the aqueous buffer portion of the solution at its working temperature for 30 min. This is meant to help the system overcome any kinetic barriers associated with being placed in a new solvent. Next, 100 mg of xylan was added, and the solution was incubated in a thermostatic shaker table at the working temperature with a rotation speed of 150 rpm. Two samples of 50 μL were extracted from the reaction solution after 24 h of reaction time. The samples were diluted 15-fold and centrifuged before they were analyzed for xylose content using HPLC or a Multiparameter Bioanalytical System. Specific details are included in the Supporting Information. The procedure was repeated for an incubated system, where the enzyme was incubated in the IL−water mixture for 24 h prior to the addition of substrate. To facilitate easy comparison across all experiments, we defined the yield of this reaction relative to the baseline case of an aqueous solution without incubation.

Dynamic Light Scattering (DLS). A Malvern Zeta Sizer ZS was used to determine the presence and size of proteins and aggregates in solution. Xylanase from *T. longibrachiatum* was obtained from Hampton Research. We chose to use an enzyme from a different supplier for the DLS studies for two reasons. First, the lyophilized enzyme used for the kinetic study displayed some aggregation even in simple PBS buffer, which was likely caused by damage due to lyophilization and rehydration. This confounded the ability of DLS to detect natively folded enzymes. Second, crystal structures of the enzyme used for DLS studies showed well-bound glycerol near the binding pocket. This had the potential to affect any kinetic studies by acting as a competitive inhibitor. The amino acid sequences of the two batches are identical, but differences in behavior can arise from the differences in preparation techniques (lyophilization vs non-lyophilization) and the mixture of other chemical additives present with the enzyme. For the DLS studies, the stock solution of xylanase was diluted 100 times to achieve a concentration of 1 mg mL^{-1} of protein in each concentration of ionic liquid. The first set of samples was allowed to sit for 30 min before sizing. A second set of samples was incubated at 310 K for 48 h. This set of samples was passed through a filter of pore size 0.64 μm, and each was allowed to sit for 30 min before sampling. All light scattering experiments were conducted five times on an individual sample at 310 K using Brand disposable UV microcuvettes, single back scattering at 173°, and viscosity and refractive index parameters obtained by linear interpolation from literature or manufacturer data.[33,34]

ASSOCIATED CONTENT

Supporting Information

This material is available free of charge via the Internet at http://pubs.acs.org

AUTHOR INFORMATION

Corresponding Author

*E-mail: jpfaendt@uw.edu.

Notes

The authors declare no competing financial interest.

■ ACKNOWLEDGMENTS

The authors acknowledge the support of NSF award CBET-1150596. This work was facilitated through the use of computational, storage, and networking infrastructure provided by the Hyak supercomputer system, supported in part by the University of Washington eScience Institute.

■ REFERENCES

(1) Garrote, G., Domínguez, H., and Parajó, J. C. (1999) Mild autohydrolysis: an environmentally friendly technology for xylooligosaccharide production from wood. *J. Chem. Technol. Biotechnol. 74*, 1101−1109.

(2) Swatloski, R. P., Spear, S. K., Holbrey, J. D., and Rogers, R. D. (2002) Dissolution of cellose with ionic liquids. *J. Am. Chem. Soc. 124*, 4974−4975.

(3) Fort, D. A., Remsing, R. C., Swatloski, R. P., Moyna, P., Moyna, G., and Rogers, R. D. (2007) Can ionic liquids dissolve wood? Processing and analysis of lignocellulosic materials with 1-n-butyl-3-methylimidazolium chloride. *Green Chem. 9*, 63−69.

(4) Li, C. L., Knierim, B., Manisseri, C., Arora, R., Scheller, H. V., Auer, M., Vogel, K. P., Simmons, B. A., and Singh, S. (2010) Comparison of dilute acid and ionic liquid pretreatment of switchgrass: Biomass recalcitrance, delignification and enzymatic saccharification. *Bioresour. Technol. 101*, 4900−4906.

(5) Wang, Y., Radosevich, M., Hayes, D., and Labbé, N. (2011) Compatible ionic liquid-cellulases system for hydrolysis of lignocellulosic biomass. *Biotechnol. Bioeng. 108*, 1042−1048.

(6) Klibanov, A. M. (2001) Improving enzymes by using them in organic solvents. *Nature 409*, 241−246.

(7) Datta, S., Holmes, B., Park, J. I., Chen, Z. W., Dibble, D. C., Hadi, M., Blanch, H. W., Simmons, B. A., and Sapra, R. (2010) Ionic liquid tolerant hyperthermophilic cellulases for biomass pretreatment and hydrolysis. *Green Chem. 12*, 338−345.

(8) Park, S., and Kazlauskas, R. J. (2003) Biocatalysis in ionic liquids−advantages beyond green technology. *Curr. Opin. Biotechnol. 14*, 432−437.

(9) Baker, G. A., and Heller, W. T. (2009) Small-angle neutron scattering studies of model protein denaturation in aqueous solutions of the ionic liquid 1-butyl-3-methylimidazolium chloride. *Chem Eng J. 147*, 6−12.

(10) De Diego, T., Lozano, P., Gmouh, S., Vaultier, M., and Iborra, J. L. (2005) Understanding structure - Stability relationships of Candida antartica lipase B in ionic liquids. *Biomacromolecules 6*, 1457−1464.

(11) Mostofian, B., Smith, J. C., and Cheng, X. (2011) The solvation structures of cellulose microfibrils in ionic liquids. *Interdiscip. Sci.: Comput. Life Sci. 3*, 308−320.

(12) Gross, A. S., Bell, A. T., and Chu, J.-W. (2011) Thermodynamics of cellulose solvation in water and the ionic liquid 1-butyl-3-methylimidazolim chloride. *J. Phys. Chem. B 115*, 13433−13440.

(13) Gupta, K. M., Hu, Z., and Jiang, J. (2011) Mechanistic understanding of interactions between cellulose and ionic liquids: A molecular simulation study. *Polymer 52*, 5904−5911.

(14) Micaelo, N. M., and Soares, C. M. (2008) Protein structure and dynamics in ionic liquids. Insights from molecular dynamics simulation studies. *J. Phys. Chem. B 112*, 2566−2572.

(15) Yon, J. M., Perahia, D., and Ghélis, C. (1998) Conformational dynamics and enzyme activity. *Biochimie 80*, 33−42.

(16) Benkovic, S. J., and Hammes-Schiffer, S. (2003) A perspective on enzyme catalysis. *Science 301*, 1196−1202.

(17) Kamerlin, S. C. L., and Warshel, A. (2010) At the dawn of the 21st century: Is dynamics the missing link for understanding enzyme catalysis? *Proteins 78*, 1339−1375.

(18) Paës, G., Tran, V., Takahashi, M., Boukari, I., and O'Donohue, M. J. (2007) New insights into the role of the thumb-like loop in GH-II xylanases. *Protein Eng., Des. Sel. 20*, 15−23.

(19) Pollet, A., Vandermarliere, E., Lammertyn, J., Strelkov, S. V., Delcour, J. A., and Courtin, C. M. (2009) Crystallographic and activity-based evidence for thumb flexibility and its relevance in glycoside hydrolase family 11 xylanases. *Proteins 77*, 395−403.

(20) Macleod, A. M., Lindhorst, T., Withers, S. G., and Warren, R. A. J. (1994) The acid/base catalyst in the exoglucanase/xylanase from Cellulomonas fimi is glutamic-acid-127 - evidence from detailed kinetic-studies of mutants. *Biochemistry 33*, 6371−6376.

(21) Turunen, O., Etuaho, K., Fenel, F., Vehmaanperä, J., Wu, X., Rouvinen, J., and Leisola, M. (2001) A combination of weakly stabilizing mutations with a disulfide bridge in the α-helix region of Trichoderma reesei endo-1,4-β-xylanase II increases the thermal stability through synergism. *J. Biotechnol. 88*, 37−46.

(22) Hakulinen, N., Turunen, O., Jänis, J., Leisola, M., and Rouvinen, J. (2003) Three-dimensional structures of thermophilic beta-1,4-xylanases from Chaetomium thermophilum and Nonomuraea flexuosa−Comparison of twelve xylanases in relation to their thermal stability. *Eur. J. Biochem. 270*, 1399−1412.

(23) Purmonen, M., Valjakka, J., Takkinen, K., Laitinen, T., and Rouvinen, J. (2007) Molecular dynamics studies on the thermostability of family 11 xylanases. *Protein Eng., Des. Sel. 20*, 551−559.

(24) Phillips, J. C., Braun, R., Wang, W., Gumbart, J., Tajkhorshid, E., Villa, E., Chipot, C., Skeel, R. D., Kalé, L., and Schulten, K. (2005) Scalable molecular dynamics with NAMD. *J. Comput. Chem. 26*, 1781−1802.

(25) Mahoney, M. W., and Jorgensen, W. L. (2000) A five-site model for liquid water and the reproduction of the density anomaly by rigid, nonpolarizable potential functions. *J. Chem. Phys. 112*, 8910−8922.

(26) Hornak, V., Abel, R., Okur, A., Strockbine, B., Roitberg, A., and Simmerling, C. (2006) Comparison of multiple amber force fields and development of improved protein backbone parameters. *Proteins 65*, 712−725.

(27) Wang, J. M., Wolf, R. M., Caldwell, J. W., Kollman, P. A., and Case, D. A. (2004) Development and testing of a general amber force field. *J. Comput. Chem. 25*, 1157−1174.

(28) Bayly, C. I., Cieplak, P., Cornell, W. D., and Kollman, P. A. (1993) A well-behaved electrostatic potential based method using charge restraints for deriving atomic charges - the RESP model. *J. Phys. Chem. 97*, 10269−10280.

(29) Ryckaert, J.-P., Ciccotti, G., and Berendsen, H. J. C. (1977) Numerical integration of the cartesian equations of motion of a system with constraints: molecular dynamics of n-alkanes. *J. Comput. Phys. 23*, 327−341.

(30) Sugahara, M., Kageyama-Morikawa, Y., and Kunishima, N. (2010) Packing space expansion of protein crystallization screening with synthetic zeolite as a heteroepitaxic nucleant. *Cryst. Growth Des. 11*, 110−120.

(31) Bernstein, F. C., Koetzle, T. F., Williams, G. J. B., Meyer, E. F., Brice, M. D., Rodgers, J. R., Kennard, O., Shimanouchi, T., and Tasumi, M. (1977) Protein Data Bank - computer-based archival file for macromolecular structures. *J. Mol. Biol. 112*, 535−542.

(32) Xu, F., Shi, Y.-C., and Wang, D. (2012) Enhanced production of glucose and xylose with partial dissolution of corn stover in ionic liquid, 1-ethyl-3-methylimidazolium acetate. *Bioresour. Technol. 114*, 720−724.

(33) Gómez, E., González, B., Calvar, N., Tojo, E., and Domínguez, Á. (2006) Physical properties of pure 1-ethyl-3-methylimidazolium ethylsulfate and its binary mixtures with ethanol and water at several temperatures. *J. Chem. Eng. Data 51*, 2096−2102.

(34) Quijada-Maldonado, E., van der Boogaart, S., Lijbers, J. H., Meindersma, G. W., and de Haan, A. B. (2012) Experimental densities, dynamic viscosities and surface tensions of the ionic liquids series 1-ethyl-3-methylimidazolium acetate and dicyanamide and their binary and ternary mixtures with water and ethanol at T = (298.15 to 343.15 K). *J. Chem. Thermodyn. 51*, 51−58.

(35) Xiong, H., Fenel, F., Leisola, M., and Turunen, O. (2004) Engineering the thermostability of Trichoderma reesei endo-1,4-β-xylanase II by combination of disulphide bridges. *Extremophiles 8*, 393−400.
(36) Bihari, M., Russell, T. P., and Hoagland, D. A. (2010) Dissolution and dissolved state of cytochrome *c* in a neat, hydrophilic ionic liquid. *Biomacromolecules 11*, 2944−2948.
(37) Sate, D., Janssen, M. H. A., Stephens, G., Sheldon, R. A., Seddon, K. R., and Lu, J. R. (2007) Enzyme aggregation in ionic liquids studied by dynamic light scattering and small angle neutron scattering. *Green Chem. 9*, 859−867.
(38) Ficke, L. E., Rodríguez, H. c., and Brennecke, J. F. (2008) Heat capacities and excess enthalpies of 1-ethyl-3-methylimidazolium-based ionic liquids and water. *J. Chem. Eng. Data 53*, 2112−2119.
(39) Menjoge, A., Dixon, J., Brennecke, J. F., Maginn, E. J., and Vasenkov, S. (2009) Influence of water on diffusion in imidazolium-based ionic liquids: a pulsed field gradient NMR study. *J. Phys. Chem. B 113*, 6353−6359.
(40) White, A. D., Nowinski, A. K., Huang, W., Keefe, A. J., Sun, F., and Jiang, S. (2012) Decoding nonspecific interactions from nature. *Chem. Sci. 3*, 3488−3494.
(41) Pollet, A., Lagaert, S., Eneyskaya, E., Kulminskaya, A., Delcour, J. A., and Courtin, C. M. (2010) Mutagenesis and subsite mapping underpin the importance for substrate specificity of the aglycon subsites of glycoside hydrolase family 11 xylanases. *Biochim. Biophys. Acta, Proteins Proteom 1804*, 977−985.
(42) Vieira, D. S., Degrève, L., and Ward, R. J. (2009) Characterization of temperature dependent and substrate-binding cleft movements in Bacillus circulans family 11 xylanase: A molecular dynamics investigation. *Biochim. Biophys. Acta, Gen. Subj. 1790*, 1301−1306.
(43) Vieira, D. S., and Ward, R. J. (2012) Conformation analysis of a surface loop that controls active site access in the GH11 xylanase A from Bacillus subtilis. *J. Mol. Model. 18*, 1473−1479.
(44) Henzler-Wildman, K. A., Thai, V., Lei, M., Ott, M., Wolf-Watz, M., Fenn, T., Pozharski, E., Wilson, M. A., Petsko, G. A., Karplus, M., Hübner, C. G., and Kern, D. (2007) Intrinsic motions along an enzymatic reaction trajectory. *Nature 450*, 838−U813.